IL NUOVO CIMENTO **45 C** (2022) 24
DOI 10.1393/ncc/i2022-22024-9

Colloquia: SoUP 2021

Simulation studies for source optimization in ^{96}Zr β decay

S. Thakur(1), V. Nanal(2)(*), Pushpendra P. Singh(1), R. G. Pillay(1), H. Krishnamoorthy(3)(4), A. Mazumdar(3)(4), A. Reza(2), P. K. Raina(1) and V. Vatsa(3)(4)

(1) *Department of Physics, Indian Institute of Technology Ropar Rupnagar, 140001, Punjab, India*
(2) *Department of Nuclear and Atomic Physics, TIFR - Mumbai, 400005, India*
(3) *India Neutrino Observatory, Tata Institute Fundamental Research Mumbai, 400005, India*
(4) *Homi Bhabha National Institute - Mumbai, 400094, India*

received 4 November 2021

Summary. — The single β decay of ^{96}Zr to the ground state of ^{96}Nb is spin forbidden and poses a great experimental challenge. The β decay of ^{96}Zr can be studied via coincident detection of de-exciting gamma rays in ^{96}Mo, which is the end product of ^{96}Nb β decay. Simulations are done with four high purity Ge (HPGe) detector setup ($\sim$ 33% relative efficiency each) to optimize the source configuration. The results suggest that $\sim$ 70 g of 50% enriched ^{96}Zr will yield sensitivity comparable to the reported results.

1. – Introduction

The ^{96}Zr is one of the two double β decay (DBD) candidates, where single β decay is spin forbidden and competes with $\beta\beta$ decay. For ^{96}Zr, $Q_{\beta\beta}$ (Q-value) is 3.35 MeV and reported limit for $T_{1/2}$ (half-life) is 3.1×10^{20} yr [1] from DBD to excited states of ^{96}Mo. A schematic representation of β decays of ^{96}Zr and ^{96}Nb is shown in fig. 1 together with prominent gamma decay cascades. There have been several attempts to measure the half-life for ^{96}Zr β decay [2-4] and the best limit is given as $T_{1/2} \geq 6.2 \times 10^{19}$ yr [5].

Given the relatively small natural isotopic abundance of ^{96}Zr (2.8 %), one of the major challenges in a rare β decay study is to improve the sensitivity, which primarily involves the reduction of background to achieve a better signal to noise ratio. Recently, an improved lower limit for $T_{1/2}$ of DBD of ^{94}Zr to excited states of ^{94}Mo has been reported using low background setup TiLES [6]. In the present work, a feasibility study of the ^{96}Zr β decay through ^{96}Mo gamma ray cascade using a low background setup of four detectors

(*) E-mail: nanal@tifr.res.in

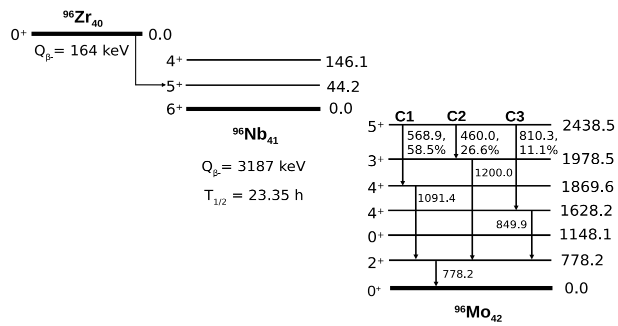

Fig. 1. – A schematic representation of β decay in ^{96}Zr and ^{96}Nb (energy values are in keV) [7].

is carried out employing the coincidence technique for background reduction. A setup of four identical HPGe detectors, with the relative efficiency of about 33%, arranged in a plane, is considered in the present study (see fig. 2). The source foil configuration and mounting geometry are optimized for maximizing the coincidence detection efficiency. The ^{96}Zr is considered to be distributed in ^{nat}Zr matrix. The results are compared with coincidence measurements of Finch *et al.* [4] with a two detector setup.

2. – Simulation and analysis

A simulation program 4HPGeSim has been developed using GEANT4 (v10.05) [8]. Figure 2 shows source and detector configuration. The geometry of the 4 HPGe detectors is taken to be similar to that of the CRADLE detector at TIFR [9], having carbon fiber housing and 0.9 mm thick front window. The source is taken to be ^{nat}Zr and effect of isotopic enrichment are taken care of by appropriately scaling the number of events generated with the desired fraction (f) while retaining the natural material properties for the source.

Two randomly oriented gamma rays from a chosen cascade (see fig. 1) are generated at a given vertex, which is uniformly distributed within the source and detected in the HPGe detectors. The dimensions of box-shaped source plates (consequently, the source mass) and their positioning are varied to find the optimum configuration to maximize mass efficiency ($M\epsilon_c$) - the product of the source mass and the coincidence photopeak efficiency. The total energy deposited in each detector (E_{dep}) is folded by a Gaussian function to account for the detector resolution and the energy detected (E_{det}) is recorded. Simulation

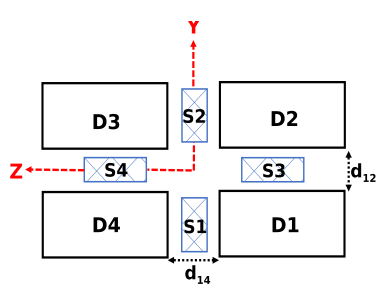

Fig. 2. – A schematic view of source - detector configuration employed in simulation.

outputs are stored and analyzed in ROOT [10] for ~ 1 M events. The photopeak area (N_i) is extracted by fitting a sum of Gaussian peaks with a quadratic background in single and coincidence spectra. The efficiency ϵ_i of detector i is given by

$$\epsilon_i = N_i/N_{gen}, \tag{1}$$

where, N_{gen} are the total generated events. The coincidence counts (N_{coin}) in the region of interest are extracted from the two dimensional correlation plots of E_i vs E_j (see fig. 3(a)). The net coincidence counts $N_{c,ij}$ are obtained after proper background and underlying Compton chance coincidence correction. The coincidence efficiency for D1-D4 and D1-D2 sets are computed as

$$\epsilon_{c,ij} = N_{c,ij}/N_{gen}. \tag{2}$$

Further, $\gamma_i - \gamma_j$ (γ_i in D4 and γ_j in D1) and $\gamma_j - \gamma_i$ (γ_j in D4 and γ_i in D1) combinations are taken into account while defining the total coincidence efficiency ϵ_c. In a rare decay experiment, the net expected event rate is often quoted in terms of $M\epsilon_c$, defined as

$$M\epsilon_c = fM_0\epsilon_c, \tag{3}$$

where M_0 is the total mass of the source, f is the isotopic fraction. It should be pointed out that with increasing thickness, the attenuation of emitted gamma rays within the source becomes increasingly important. Hence, the source geometry needs to be optimized to maximize $M\epsilon_c$. Initially, $M\epsilon_c$ is optimized for a two detector setup D1-D4 (front source) and D1-D2 (side source). For the front source, thickness t is varied, keeping the cross-sectional area of ($l \times w$) constant. For the side source, both thickness t and width w are varied, keeping l constant and the effect of variation of l is investigated separately. Distance between detectors d_{12}/d_{14} is fixed at $t + 10$ mm.

3. – Results and discussion

Amongst all 3 possible $\gamma - \gamma$ combinations in the most dominant cascade C1 (see fig. 1), 568–1091 keV pair is expected to give a cleaner identification of the decay branch. Hence the source geometry optimization has been done for this pair. For side source, it is observed that both singles and coincidence efficiencies show weak dependence on the source width. As no significant gain in $M\epsilon_c$ was observed for $w > 30$ mm, w_{opt} is taken to be 30 mm. The optimal source length (l_{opt}) is taken to be 55 mm same as the crystal length. The $M\epsilon_c$ for 568-1091 keV gamma pair are plotted as a function of source thickness in fig. 3(b) for front and side sources. As expected, for the given mass of the source, the side configuration yields lower efficiency ($\sim$half) as compared to the front source. For 778–1091 keV pair, as energy is higher, the optimal thickness is somewhat higher than 10 mm. Although the highest $M\epsilon_c$ is observed for the 568–778 keV pair, the background in the relevant region will be a crucial factor in the actual experiment. The optimal source dimensions for 2 detector setup are 55 mm$\times$55 mm$\times$10 mm and 55 mm$\times$30 mm$\times$10 mm for front and side source, respectively. These are used in optimizing the 4 detector setup. To compare the present $M\epsilon_c^{opt}$ with the earlier measurement of Finch et al. [4], $M\epsilon_c$ is estimated for 568-1091 keV gamma ray pair for the reference source-detector geometry. Two coaxial HPGe detectors with ~ 88 mm diameter (dia) and ~ 50 mm length, having 2.54 mm thick magnesium front window are mounted

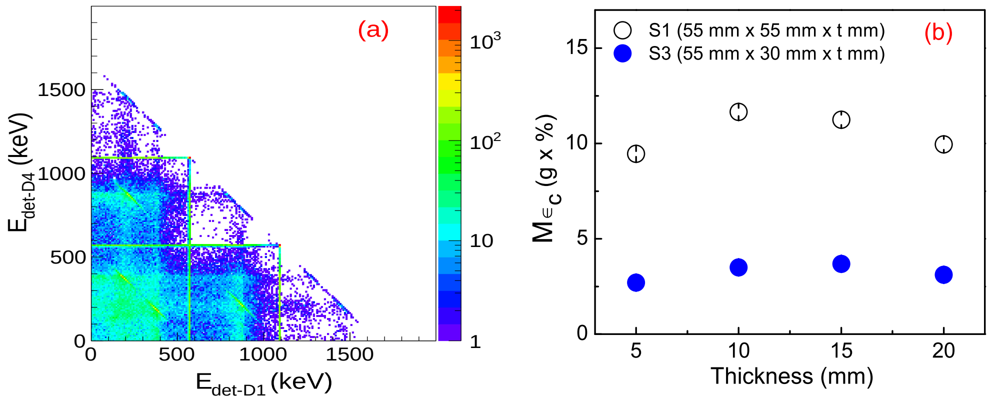

Fig. 3. – (a) Simulated 2D spectrum of the detected energy in D1 and D4, (b) Simulated Mϵ_c for 568-1091 keV gamma rays as a function t for both front (S1) and side (S3) Zr sources.

face to face at a distance (d) of 12 mm. A cylindrical source of mass $\sim$36.8 g with $\sim$50 % enrichment and $\sim$60 mm dia×2 mm size is considered, giving $M_{ref} \sim 18$ g of ^{96}Zr. As it can be seen from table I, a significantly large quantity of the Zr source will be needed to achieve Mϵ_c similar to earlier measurement with present set of detectors. It should be mentioned that the measured best reported limit so far on $T_{1/2}$ of ^{96}Zr employed about 19 g of ZrO_2 powder with 57.3 % enrichment for singles gamma ray measurements, resulting in Mϵ of $\sim$37 g-% [2].

For the four detector setup, the total mass is configured in four sources - S1+S2 (front sources) and S3+S4 (side sources). Initially, the respective optimum source dimensions obtained in the two detector geometry for the front (55 mm×55 mm) and side sources (55 mm×30 mm) are employed and sources are positioned symmetrically w.r.t detector crystal for better solid angle coverage. It may be noted that reducing thickness t from 10 mm to 5 mm, permits $d_{14} = 7$ mm, which yields $\sim$60 % gain in ϵ_c. Thus, even though there is a mass decrease of 50 %, only $\sim$20 % decrease is observed in the total Mϵ_c. The four detector configuration with t = 5 mm for front and side sources will result in 70 % higher Mϵ_c (see table I), but still considerably large mass $\sim$152 g of ^{96}Zr will be needed. Hence, further mass optimization needs to be considered.

As mentioned earlier, dominant contribution comes from sources in the front. So in the first step, only front sources S1 and S2 are employed and the cross-sectional area of the source ($l \times w$) is varied, maintaining $t_0 = 5$ mm and d = 7 mm to obtain the optimal front source mass (M_f). In the second step, a fraction of M_f (30-60 %) is distributed as side sources S3 and S4. Similar to the first case, t_0 and d are kept as 5 mm and

Table I. – *A comparison of Mϵ_c (568-1091) for D1-D4 and ref.* [4] *setup ($f = 50$ %).*

Crystal size	Front window (mm)	Source size	d (mm)	ϵ_c %	M (g)	Mϵ_c (g-%)
88 mm (dia)×50 mm	2.54	60 mm (dia)×2 mm	12	0.65	18	12
55 mm (dia)×55 mm	0.90	55 mm×55 mm×2 mm	12	0.12	20	2

TABLE II. – $M\epsilon_c(\gamma_1, \gamma_2)$ *in optimal source configuration* ($M_{eff} \sim 72$ g) *in 4 detector geometry.*

Eγ (keV)	ϵ_c (%)	Mϵ_c (g-%)
568, 1091	0.216	15.4
568, 778	0.279	20.0
778, 1091	0.172	12.3

7 mm, respectively, and ($l \times w$) is varied keeping M$_f$ fixed ($l <$ crystal length, to avoid edge effects). The optimal configuration for t = 5 mm is obtained as $M_{eff} \sim 72$ g with M$_s \sim 40$ % of M$_f$. The cross-sectional dimensions (l_{opt}, w_{opt}) are 40 mm×40 mm for the front source and 30 mm×20 mm for the side source. The M$\epsilon_c(\gamma_1, \gamma_2)$ in Zr matrix with ~ 50 % enrichment for the optimal source configuration are given in table II. Although higher granularity in the four detector setup is expected to improve the background and reduce the pileup, these effects cannot be quantified at this stage.

4. – Conclusion

Simulation studies are carried out for estimation of mass efficiency (Mϵ_c) for β decay measurements in ^{96}Zr. The optimization of Mϵ_c is done for four HPGe detector (~ 33 % relative efficiency each) setup with extended sources in a close geometry for 568-1091 keV gamma ray pair in the ^{96}Nb decay cascade. It is shown that for ^{96}Zr β decay, even in a four detector configuration, a significantly larger source mass is required to achieve the reported sensitivity. Present simulations for a four detector setup show the optimal source configuration to be 5 mm thick foils with a cross-sectional area of 40 mm×40 mm for front sources and 30 mm×20 mm for side sources. This corresponds to about 72 g of effective mass with 50 % enrichment and can yield Mϵ_c of $\sim$12-20 g-% for different gamma ray pairs, which is slightly better than the coincidence measurement reported earlier.

* * *

This work is supported by the Department of Atomic Energy, Government of India (GoI), under Project No. 12-R&DTFR-5.02-0300. S. Thakur acknowledges the Ministry of Education, GOI, for PhD research fellowship, and TIFR for supporting the visit related to this work.

REFERENCES

[1] Finch S. W. *et al.*, *Phys. Rev. C*, **92** (2015) 045501.
[2] Arpesella C. *et al.*, *Europhys. Lett.*, **27** (1994) 29.
[3] Barabash A. S. *et al.*, *J. Phys. G: Nucl. Part. Phys.*, **22** (1996) 487.
[4] Finch S. W. *et al.*, *Nucl. Instrum. Methods A*, **806** (2016) 70.
[5] Mayer A. J. *et al.*, *Phys. Rev. C*, **98** (2018) 024617.
[6] Dokania N. *et al.*, *Eur. Phys. J. A*, **53** (2017) 270.
[7] `https://www.nndc.bnl.gov/`.
[8] Agostinelli S. *et al.*, *Nucl. Instrum. Methods A*, **506** (2003) 250.
[9] Gupta G. *et al.*, *DAE-BRNS Symp. Nucl. Phys.*, **63** (1142) 2018.
[10] Brun R. *et al.*, *Nucl. Instrum. Methods A*, **389** (1997) 81.